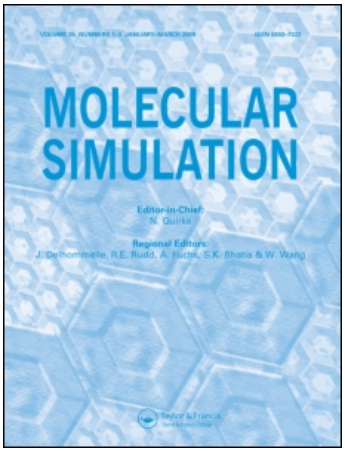

Molecular Simulation
Publication details, including instructions for authors and subscription information:
http://www.informaworld.com/smpp/title~content=t713644482

Mesoscale Modelling

David Nicolaides[a]
[a] Molecular Simulations Ltd, Cambridge, United Kingdom

To cite this Article Nicolaides, David(2001) 'Mesoscale Modelling', Molecular Simulation, 26: 1, 51 — 72
To link to this Article: DOI: 10.1080/08927020108024200
URL: http://dx.doi.org/10.1080/08927020108024200

Molecular Simulation, 2001, Vol. 26, pp. 51–72
Reprints available directly from the publisher
Photocopying permitted by license only

MESOSCALE MODELLING

DAVID NICOLAIDES*

Molecular Simulations Ltd, The Quorum, Barnwell Road, Cambridge CB5 8RE, United Kingdom

(Received March 1999; accepted June 1999)

Increasingly, industrial materials are being designed to have structure on length scales of tens to thousands of nanometers. These structures are crucial to achieving a particular desired material property. Such structures, however, may depend on the underlying chemistry of the material for their existence. For example, a thousandfold increase in the ionic conductivity of a polymer blend may only occur in a narrow region of a hugely complex phase diagram, the location of which region can be expected to depend on the molecular chemistry and physics from the monomer scale to the coil size.

Traditional Computational Chemistry has proved incapable of dealing with the length and time scales involved in the formation of these 'Mesoscale' structures. On the other hand, traditional Computational Physics has proved incapable of consistently incorporating the necessary chemical detail for modelling real industrial materials. In this paper we present two novel methods which successfully address both the chemistry and the physics of mesophase formation. The methods, described in detail, are MesoDyn and Dissipative Particle Dynamics (DPD).

Unlike phenomenological theories of materials, such as the Landau models which one finds in much of the computational physics literature, the two models mentioned incorporate molecular geometry and connectivity explicitly. We discuss each of the methods briefly.

We then give an overview of how these methods are being used in industry to optimise materials and processes. We discuss previous simulation results for triblock Pluronic surfactants in solution studied with MesoDyn, and for diblock copolymers studied with DPD, where the known experimental changes in morphology from micellar to hexagonal to bicontinuous to lamellar have been successfully reproduced. We also present new results for several systems, including binary and ternary blends, where the third component in the latter system is a diblock copolymer, which acts as a compatibiliser. We discuss the effects of changing solvent character on the material properties of these systems, as well as the effects of an externally imposed shear flow.

Keywords: Soft condensed matter; Polymers; Phase separation

*e-mail: dnicolaides@msicam.co.uk

INTRODUCTION

MesoDyn and Dissipative Particle Dynamics (DPD) are new tools for the prediction of mesoscale structures of soft condensed matter. These are the patterns of size 10 to 100 nm which can be found for example in polymer blends, block-copolymer systems, surfactant aggregates in detergent materials (*e.g.*, shampoo), latex particles, or drug delivery systems. In contrast to previous approaches aiming at classifying such morphologies by means of equilibrium theories, the present approaches recognise the fact that by their very nature these patterns are irregular, and hence can only be characterised *via* the dynamic properties of the systems. From an industrial perspective this approach is much more realistic, since typical processing times are orders of magnitude shorter than the thermodynamic relaxation time and thus such non-perfect states contribute substantially to the behaviour of the final material. A typical scenario is that of a quenched block-copolymer melt which rapidly undergoes an initial phase separation ('spinodal decomposition'), but subsequently gets stuck in a defect-rich morphology, *i.e.*, not reaching thermodynamic equilibrium.

MesoDyn and DPD aim to bridge the gap between the fast molecular kinetics on the one hand, and the slow thermodynamic relaxation of macroscale properties on the other. This is done by means of a well-defined coarse grained representation of the molecular model which forms the basis of a simulation of the phase separation process leading to mesoscale morphologies. These can then be linked to macroscale properties.

The molecules are defined on a coarse-grained level as 'chains of beads'. Each bead is of a certain component type representing covalently bonded groups of atoms such as a few monomers of a polymer chain, also known as a Kuhn or statistical segment. Chemically specific information about the molecular ensemble enters into MesoDyn and DPD *via* material parameters such as the bead-bead (Flory-Huggins) interaction parameters, the bead sizes and the molecular architecture (chain length, branching *etc.*). At this point, the two methods diverge, in that they treat the dynamics of the system differently. The dynamics of the system in MesoDyn is described by a set of so-called functional Langevin equations. In simple terms these are diffusion equations in the component densities which take account of the noise in the system. By means of numerical inversions, the evolution of the component densities is simulated, starting from an initially homogeneous mixture in a cube of typical size 50 – 100 nm and with periodic boundary conditions. The dynamics of the system in DPD is described by explicit equations of motion for the beads, chosen so as to reproduce Navier-Stokes hydrodynamics in

the large. Both methods are described more fully in the Theory section below. Component density fields can be recovered from DPD by a suitable local averaging.

The ensuing mesoscale phase separated morphologies can be analysed in the commercial Cerius[2] software of Molecular Simulations Inc, by means of slices through the cubic box, or display of isodensity surfaces. The simulation results can also be compared directly with experimental observations *e.g.*, from electron microscopy or X-ray scattering. The method allows one to assess the effects of changes to the molecular composition of a formulation on the microstructure and hence the expected macroscopic properties.

The present paper briefly reviews the underlying theory behind the two methods, then focuses on applications of interest to industry.

THEORY

MesoDyn

MesoDyn is based on a dynamic variant of mean-field density functional theory [1–2]. The latter is based on a theorem which essentially states that there is a one-to-one mapping between the component densities in a system and their conjugate external potential fields. Furthermore, a real system, *i.e.*, a system with interactions, can be equated to an *ideal* system, *i.e.*, without interactions, *via* a set of effective external potentials. The reason for this is that with the above theorem external potentials can always be found such that the probability distribution functions of the ideal system equal that of the real system at the same densities.

This theory can be used to great effect in the description of polymer fluids. We take the polymer chain as the fundamental building blocks of the model. In this description, the intrachain correlations can in principle be treated by any suitable model. In practice, a Gaussian chain model is used (a) because it allows a factorization of the interactions, hence is computationally very efficient, and (b) because it can be shown that the Gaussian chain may be used as a statistical model for a real chain, *i.e.*, for each real, atomistic force-field model, a Gaussian chain representation with the same response function can be found. The non-interacting Gaussian chains are hence the *ideal* system. Any interchain, *i.e.*, non-bonded interactions are treated as *non-ideal*, *i.e.*, they enter into the effective external potential.

Hence, the molecular ensemble is represented by a number n of Gaussian chains, made up of a number of different beads of types I, with a total number of N beads per chain. At an instant of time there will be a certain

probability distribution Ψ of bead positions in space, resulting in a three-dimensional concentration fields $\rho_I(\mathbf{r})$. The evolution of these fields is the result of the dynamics outlined in the following subsection, in combination with the thermodynamic driving force described in the section thereafter. For simplicity of the presentation, in the following we are going to limit the number of bead types to two, named A and B, but the theory will equally apply to any number of bead types.

MesoDyn Dynamics

The derivation of the diffusive dynamics of the molecular ensemble is based on the assumption that for each type of bead I the local flux is proportional to the local bead concentration and the local thermodynamic driving force:

$$\mathbf{J}_I = -M\rho_I \nabla \mu_I + \tilde{\mathbf{J}}_I \tag{1}$$

where $\tilde{\mathbf{J}}_I$ is a stochastic flux (related to noise). Together with the continuity equation

$$\frac{\partial \rho_I}{\partial t} + \nabla \cdot \mathbf{J}_I = 0 \tag{2}$$

this leads to simple diagonal functional Langevin equations (stochastic diffusion equations) in the density fields:

$$\frac{\partial \rho_I}{\partial t} = M\nabla \cdot \rho_I \nabla \mu_I + \eta_I \tag{3}$$

with a Gaussian distribution of the noise η_I. The original method modified Eq. 3, introducing 'exchange' Langevin equations to account for the near-incompressibility of a polymer melt or solution [2]: however, subsequent work has allowed for a description of compressibility effects *via* the thermodynamics of the model [3], which is described in the next subsection.

Here M is a bead mobility parameter. The kinetic coefficient $M\rho_I$ models a local exchange mechanism. Hence the model is strictly valid only for Rouse dynamics. (Effects such as reptation lead to kinetic coefficients which extend over a range of roughly the coil size. They lead to computationally expensive non-local operators which in addition, are very complex in the non-linear regime.) However, by rewriting the diffusion equation in terms of the potential field conjugate to the density field, reptation effects can be included in a simple manner [4].

MesoDyn Thermodynamics

The above Langevin equations contain the bead chemical potential as the thermodynamic driving force of the diffusive dynamics. These chemical potentials can be derived from the thermodynamics of the molecular ensemble.

The first step is to derive an expression for the free energy of the system in terms of the bead distribution functions Ψ. Since the positions of the beads are correlated to each other this amounts to a multi-dimensional many-body problem. To overcome this, any interchain correlations are neglected and the system is approximated by a set of independent Gaussian chains embedded in a mean-field.

The distribution functions of the independent Gaussian chains factorize exactly and hence the density functional can be simplified to a product of single-chain density functionals. In this approximation, the free energy functional can be written as

$$F[\Psi] = \frac{1}{Q}\int d\mathbf{R}\left(\Psi H^{id} + \frac{1}{\beta}\Psi \ln \Psi\right) + F^{nid}[\Psi] \tag{4}$$

The first term is the average value of the Hamiltonian for the ideal system, comprising the internal Gaussian chain interactions:

$$H^{id} = \sum_{\gamma=1}^{n} H_{\gamma}^{G} \tag{5}$$

where H_{γ}^{G} is the Gaussian chain Hamiltonian of chain γ:

$$\beta H_{\gamma}^{G} = \frac{3}{2a^2}\sum_{s=2}^{N}\left(\mathbf{R}_{\gamma s} - \mathbf{R}_{\gamma s-1}\right)^2 \tag{6}$$

here a is the Gaussian bond length parameter and the index s goes over all N segments of the chain. The second term in the free energy functional stems from the Gibbs entropy of the distribution. The third term is the non-ideal contribution related to the interchain interactions. In the present mean-field approximation the latter is independent of the particular distribution Ψ. In the spirit of the particular application of density functional theory taken here, namely treating the chains as the ideal system, the correlations between the chains are neglected and the density functional method applies to the correlations within the Gaussian chain only.

The key ansatz of dynamic density functional theory is now that on a coarse-grained time-scale the distribution function Ψ is such that the free

energy functional $F[\Psi]$ is constantly minimized. Hence Ψ is independent of the history of the system, and is fully characterized by the constraints that it represents the density distribution and minimizes the free energy functional. This constraint on the density fields is realized by means of an external potential U_I.

The constrained minimization of the free energy functional leads to an optimal distribution, which in turn, and by the one-to-one relation between densities, distributions and external potential can be written as:

$$\beta F[\rho] = n \ln \Phi + \ln n! - \sum_I \int U_I(\mathbf{r}) \rho_I(\mathbf{r}) d\mathbf{r} + \beta F^{nid}[\rho] \tag{7}$$

where a Flory-Huggins type interaction is introduced for the non-ideal (inter-chain) interactions:

$$\begin{aligned} F^{nid}[\rho] = \frac{1}{2} \int \int & \varepsilon_{AA}(|\mathbf{r} - \mathbf{r}'|) \rho_A(\mathbf{r}) \rho_A(\mathbf{r}') + \varepsilon_{AB}(|\mathbf{r} - \mathbf{r}'|) \rho_A(\mathbf{r}) \rho_B(\mathbf{r}') \\ & + \varepsilon_{BA}(|\mathbf{r} - \mathbf{r}'|) \rho_B(\mathbf{r}) \rho_A(\mathbf{r}') + \varepsilon_{BB}(|\mathbf{r} - \mathbf{r}'|) \rho_B(\mathbf{r}) \rho_B(\mathbf{r}') \end{aligned} \tag{8}$$

where $\varepsilon_{IJ}(|\mathbf{r} - \mathbf{r}'|)$ is a mean-field energetic interaction between beads type I at $\mathbf{r}$ and J at $\mathbf{r}'$, defined by the same Gaussian kernel as in the ideal chain Hamiltonian

$$\varepsilon_{IJ}(|\mathbf{r} - \mathbf{r}'|) = \varepsilon_{IJ}^0 \left(\frac{3}{2\pi a^2} \right)^{3/2} \exp \left[-\frac{3}{2a^2} (\mathbf{r} - \mathbf{r}')^2 \right] \tag{9}$$

MesoDyn Numerics

The Gaussian chain density functional constitutes a one-to-one relation between the external potential fields and the density fields for each bead type. In addition, the intrinsic chemical potentials μ_I are functionals of the external potentials and the density fields. The coupled Langevin equations constitute a relation between the time derivatives and the intrinsic chemical potentials. Finally, the noise source is related to the exchange kinetic coefficients by the fluctuation-dissipation theorem. Together these equations form a closed set, which can be integrated efficiently on a cubic mesh by a Crank-Nicholson scheme.

Since a very large number of equations (about 10^6 nested Fredholm integrals per time step) has to be solved and memory requirements for systems of up to 10 beads on meshes of the order of 100^3 is also very high, a domain decomposition has been method has been used and implemented

using the industry standard MPI (Message Passing Interface) for parallel platforms with distributed memory.

DPD

Some years ago, Hoogerbrugge and Koelman [5] introduced a new simulation technique, derived from Molecular Dynamics simulations and Lattice Gas Automata, that was based on the idea of integrating the equations of motion for particles, but integrating out the smallest spatial degrees of freedom first. The fast motion of the atoms in a system is averaged over and the remaining structure is represented by a set of "beads", of given mass and size, that interact *via* soft potentials with other beads. A bead represents a small region of soft matter and its motion is assumed to be governed by Newton's laws in which the total force allows one to integrate its equations of motion. The forces must be carefully chosen so as to reproduce fluctuating hydrodynamics in thermal equilibrium for the system as a whole. In the following two subsections we describe briefly how this is done and how the original theory can be extended to implement an off-lattice version of the Flory-Huggins theory of polymeric fluids [8].

DPD Dynamics

DPD beads interact by specified forces which determine their dynamics:

$$\frac{\partial \mathbf{r}_i}{\partial t} = \mathbf{v}_i, \quad m_i \frac{\partial \mathbf{v}_i}{\partial t} = \mathbf{f}_i, \tag{10}$$

where $\mathbf{r}_i$, $\mathbf{v}_i$ and $\mathbf{f}_i$ are the position vector, velocity and total force on the ith bead. For simplicity, we set all bead masses m_i equal to unity.

Each bead is subject to three forces from its neighbors: a conservative interaction which is linear in the bead–bead separation; a dissipative force proportional to the relative velocity of two beads and a random force between a bead and each of its neighbors. The need for these three forces may be understood qualitatively by imagining trying to push two beads, or 'fluid droplets' together. In doing so one will certainly experience repulsive forces, however these will be much softer than the dispersive forces between atoms. One will also encounter viscous forces and, if the droplets are small, Brownian forces. The essential ingredient in getting the total force on a bead correct is to determine the relative strengths of the three individual forces. A key step in this was the work of Warren and Espanol in using the fluctuation-dissipation theorem to relate the coefficients of the dissipative and random forces [6].

The total force on a bead is thus expressed as

$$\mathbf{f}_i = \sum_{j \neq i} (\mathbf{F}_{ij}^C + \mathbf{F}_{ij}^D + \mathbf{F}_{ij}^R), \tag{11}$$

where the sum is over all beads within a distance r_c of the ith bead. This short-range cut-off makes the interactions local. It is convenient to set r_c equal to unity so that all lengths are measured relative to the bead radius. The conservative force is a repulsive central force with a maximum magnitude given by the so-called repulsion parameter a_{ij}

$$\mathbf{F}_{ij}^C = \begin{cases} a_{ij}(1 - r_{ij})\hat{\mathbf{r}}_{ij} & r_{ij} < 1 \\ 0 & r_{ij} > 1, \end{cases} \tag{12}$$

where r_{ij} is the magnitude of the bead–bead vector $\mathbf{r}_{ij}$, and $\hat{\mathbf{r}}_{ij}$ is the unit vector joining beads i and j.

The dissipative force is proportional to the relative velocity of two beads and acts so as to reduce their relative momentum.

$$\mathbf{F}_{ij}^D = \begin{cases} -\gamma(\omega(r_{ij}))^2(\hat{\mathbf{r}}_{ij} \cdot \mathbf{v}_{ij})\hat{\mathbf{r}}_{ij} & r_{ij} < 1 \\ 0 & r_{ij} > 1, \end{cases} \tag{13}$$

where $\omega(r_{ij})$ is a short-range weight function. Because of the pairwise form chosen for the dissipative force it conserves the total momentum of each pair of particles and hence also of the system. This is what gives hydrodynamic behaviour to the system, as opposed to the Brownian Dynamics simulation method, where the dissipative forces on the particles act with respect to a fixed external reference frame.

The random force also acts between all pairs of beads subject to the same short-range cut-off and acts so as to pump energy into the system

$$\mathbf{F}_{ij}^R = \begin{cases} \sigma\omega(r_{ij})\zeta_{ij}\hat{\mathbf{r}}_{ij} & r_{ij} < 1 \\ 0 & r_{ij} > 1, \end{cases} \tag{14}$$

where $\zeta_{ij}(t)$ is a delta-correlated stochastic variable with zero mean.

DPD Thermodynamics

The thermodynamics of DPD was studied by Groot and Warren [7], among others, who found from simulations that for moderate densities

(approximately 3–10 beads per unit volume of the simulation box) and repulsion parameters ($a = 15-30$) the equation of state of a simple DPD fluid is

$$p = \rho k_B T + \alpha a \rho^2 \tag{15}$$

where p is the pressure, ρ is the density and $\alpha = 0.101 \pm 0.001$. The magnitude of the repulsion parameter can thus be fixed by requiring the dimensionless compressibility of the DPD fluid to be equal to that of water.

Groot and Warren also extended the DPD method to polymeric systems, by including harmonic forces between beads, as with the Gaussian Chain molecular model used in MesoDyn and in fact considered multicomponent polymeric systems, where we expect a correspondence with Flory-Huggins theory [8].

The free energy density of a single-component DPD fluid whose equation of state, as given above, is quadratic in the density is

$$\frac{f_v}{k_B T} = \rho \ln \rho - \rho + \frac{\alpha a \rho^2}{k_B T}, \tag{16}$$

and for a two-component fluid we expect

$$\begin{aligned} \frac{f_v}{k_B T} = {} & \frac{\rho_A}{N_A} \ln \rho_A - \frac{\rho_A}{N_A} + \frac{\rho_B}{N_B} \ln \rho_B - \frac{\rho_B}{N_B} \\ & + \frac{\alpha}{k_B T} (a_{AA} \rho_A^2 + 2 a_{AB} \rho_A \rho_B + a_{BB} \rho_B^2). \end{aligned} \tag{17}$$

This is of the Flory-Huggins form, provided we identify the χ parameter as

$$\chi = \frac{2\alpha (a_{AB} - a_{AA})(\rho_A + \rho_B)}{k_B T}. \tag{18}$$

Groot and Warren (1997) found the χ parameter to be proportional to $(a_{AB} - a_{AA})$ as predicted by Eq. 18, but the constant of proportionality α is not linear in the density:

$$\begin{aligned} \chi &= (0.286 \pm 0.002)(a_{AB} - a_{AA}) \\ \chi &= (0.689 \pm 0.002)(a_{AB} - a_{AA}), \end{aligned} \tag{19}$$

for densities of $\rho = 3$, 5 respectively. Nonetheless, such a relation can be measured from a set of simulations at a fixed density and used to relate the

repulsion parameters in the DPD fluid to the χ parameter in the Flory-Huggins theory.

APPLICATIONS

MesoDyn

The MesoDyn code has been applied by workers at the University of Groningen to study the microphase separation dynamics of aqueous solutions of specific triblock surfactants (tradename Pluronic), which are used as emulsifiers, stabilisers, and wetting and drug delivery agents [9–12]. These are nonionic copolymers, with poly(ethylene-oxide) (PEO) blocks on the outside and poly(propylene-oxide) (PPO) blocks in the middle, and come in a range of molecular weights.

For the Pluronic L64, four different mesophase morphologies are known to exist in a small 50–70% surfactant concentration interval [9]. All four different phases (micellar, hexagonal, bicontinuous and lamellar) including their defects and time development are reproduced in MesoDyn simulations (see Fig. 1), which is in excellent agreement with experiments [10]. In a further study, using the same parameters, the known phase behaviour of the Pluronic 25R4 was equally well reproduced [10].

A further study of these systems under the influence of shear has clarified the complex interplay between the phase separation dynamics and the dynamics imposed by the flow. These are the first 3-dimensional computer simulations of morphology formation in *specific* polymer surfactant solutions. Until now, existing methods to predict morphologies in complex liquids did not provide an efficient way to couple molecular properties to the microphase behaviour. The MesoDyn code provides a flexible way to account for changes in molecule properties, such as changes in the block lengths and the chemical dissimilarity between blocks.

Scientists at BASF have used MesoDyn to model a range of diblock surfactants in solution; the ultimate aim is to gain enough of a quantitative understanding of specific surfactants to improve long-standing industrial processes such as emulsion polymerisation [12].

MesoDyn is able to clarify the complex behaviour which occurs in the early stages of latex particle formation. This part of the process is largely out of range of experiments, as it is so short-lived. The goals are to first control micelle size and polydispersity, which in turn affect the polymerisation process and the final particle size distribution, and second to determine how the structure affects the final material properties of the latex.

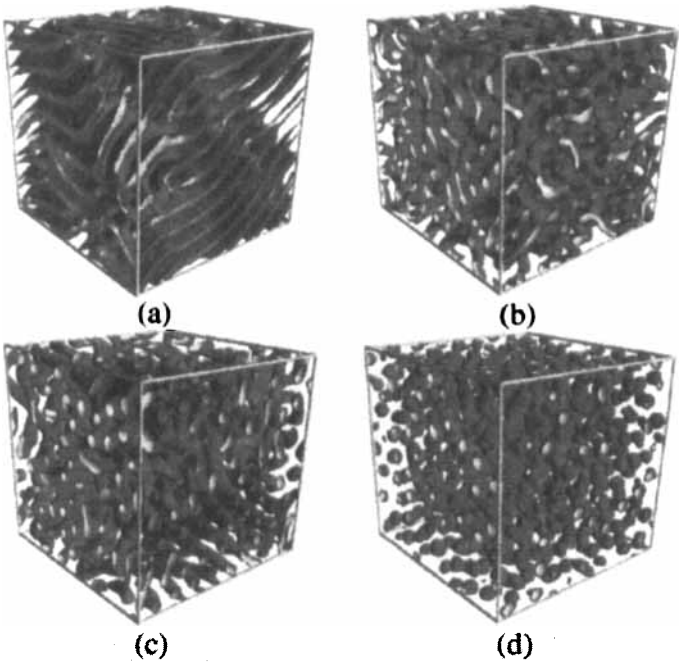

FIGURE 1 Morphology of Pluronic L64 solutions at 70% (a), 60% (b), 55% (c) and 50% (d) concentration. In exact agreement with experiment, the morphologies are seen to be lamellar, bicontinuous, hexagonal and micellar, respectively. (See Color Plate VII).

A key first step was in understanding how hydrophilic block length in the nonionic surfactants which are commonly used (such as Lutensol, a BASF product), can best be engineered for maximum micelle stability and monodispersity. Simulations revealed that increasing the block length both reduced micelle coagulation and decreased polydispersity (see Fig. 2a). This can be subsequently understood as allowing a better balancing of the Laplace pressure arising from the micelle curvature. However, this was found to happen only for a range of interaction parameters; when the interaction strengths of the hydrophobic blocks with water became too large, the micelle size distribution become bimodal (Fig. 2b).

At high concentrations, an inversion of the micelles is seen, where water droplets, or inverse micelles, form (see Fig. 3). These then coalesce, in order to lower their free energy by sharing unfavourable surface area.

At Molecular Simulations, studies with MesoDyn have included the effects of solvent quality on the diblock copolymer phase diagram, and the compatibilisation of polymer blends.

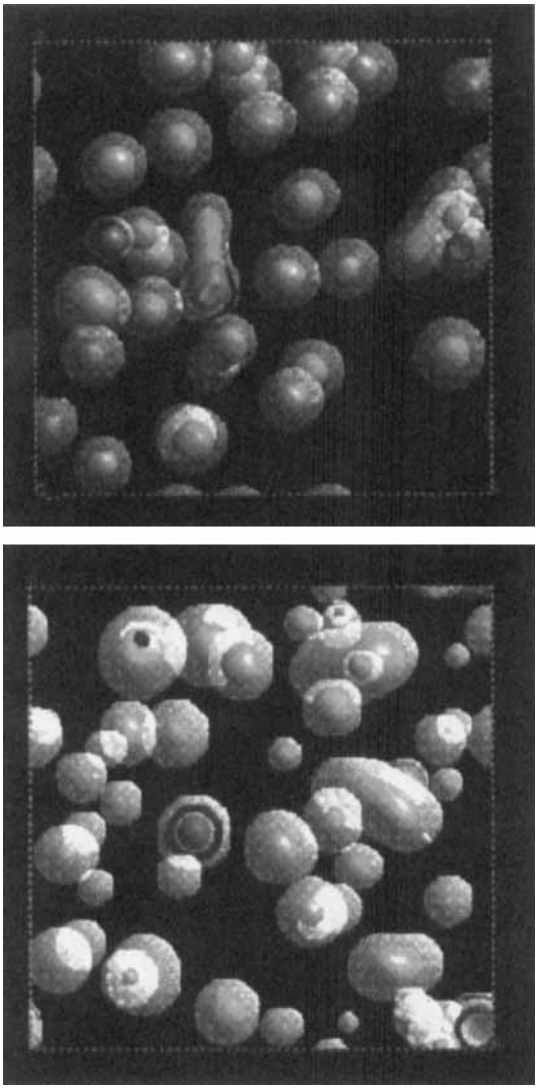

FIGURE 2 (a) Morphology of micellar surfactant phases with a controlled degree of polydispersity. The efficient packing of the higher molecular weight surfactant tails into the micelle core is seen. This gives rise to a very uniform micelle size distribution. (b) When the hydrophobicity of the surfactant tails is increased beyond a certain point, the size distribution becomes bimodal. (See Color Plate VIII).

In the first case, a recent experimental study of polystyrene-polyisoprene (PS-PI) diblocks in the selective solvent di-*n*-butyl phthalate (DNBP) was taken as the starting point [13]. The effects of a solvent on the morphology

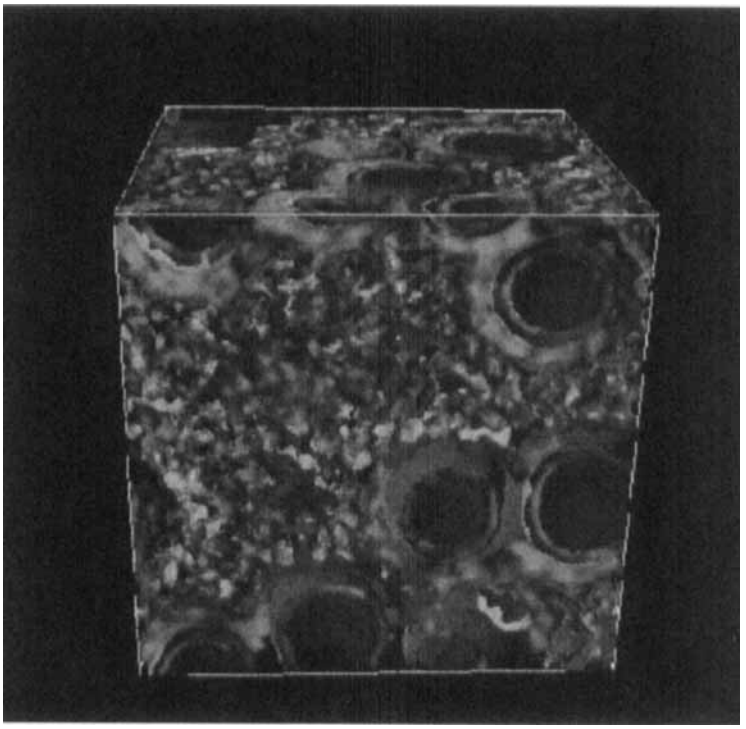

FIGURE 3 Iso-density surfaces of the hydrophobic B beads (yellow), hydrophilic A beads (red) and water (blue), of an A_2B_8 70% solution. The water forms reverse micelles, which then coalesce in order to reduce unfavourable surface area. (See Color Plate IX).

can be rationalised to a first approximation by considering the amount by which the relative sizes of the two blocks are modified from the polymer in the melt. The equilibrium phase diagram of a pure diblock copolymer melt has been mapped out by self-consistent field methods, and is shown in Figure 4 [14]. The two state variables are χN, the Flory-Huggins parameter times the overall polymer length N, and f, the block fraction of one of the components. In the present case, the DNBP stretches the PS block, while compacting the PI block, giving rise to a polymer with an effective f which is radically different to that of the polymer in the melt. In the melt, the PS-PI polymers were known to order into a micellar phase with the PS in the micelle core; the experimental results of reference 13 predicted for a 70% solvent concentration either a hexagonal (rod) phase, with the PI as the minority component (*i.e.*, in the middle of the rods), or possibly a lamellar phase. The simulation results, which had essentially no free parameters, showed a morphology which was complex, but with strong lamellar

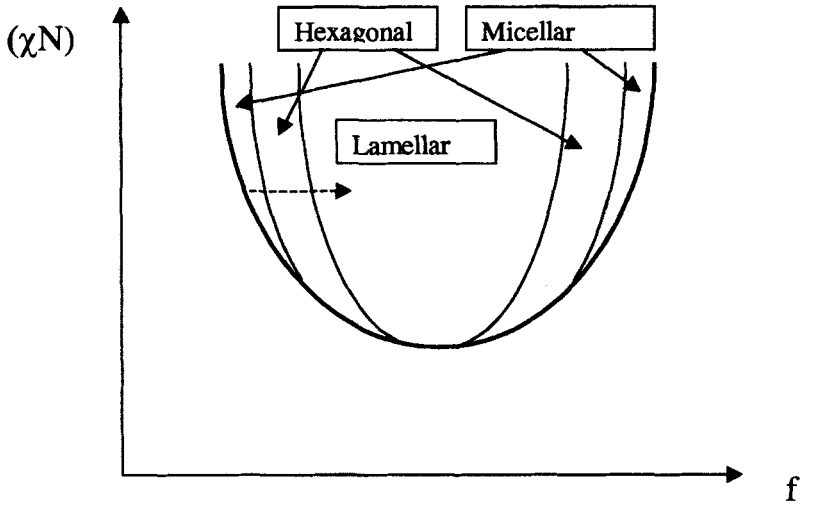

FIGURE 4 Schematic drawing of the *AB* diblock copolymer phase diagram, as calculated using a self-consistent field method. For the full diagram, see Reference 15. The state variables are χN, the Flory-Huggins χ parameter times the total polymer length, and f, the fraction of the polymer which is of type *A*. The effects of the selective solvent di-*n*-butyl phthalate on a polystyrene-polyisoprene diblock copolymer are to shift the phase diagram, as represented by the dotted arrow.

features. Upon shearing the system, it was seen to evolve into a morphology with coexisting hexagonal and lamellar phases (see Fig. 5). Such a coexistence of two morphologies has also been seen in recent simulations of the Pluronics by the University of Groningen [15].

In the studies of blend compatibilisation, the work focused on quantifying the mechanisms of compatibilisations, and improving blend formulation. In the early work of Leibler [16], two mechanisms were suggested: interfacial adsorption and solubilisation. Our work suggests that for high molecular weight PS-PI blends with a diblock PS-PI compatibiliser, only the first mechanism is significant. The benefits of compatibilisation are obvious from comparison of Figure 6a, which represents a system without compatibiliser, to Figure 6b, which represents a system with a compatibiliser of the same molecular weight as the homopolymers (80,000 g/mol) at the same time after demixing has started. The addition of compatibiliser lowers the interfacial tension, and stabilises surfaces with significantly higher curvature. The amount of decrease in the surface tension can be estimated roughly by using Gibbs adsorption equation,

$$d\gamma = -\Gamma_c d\mu_c \tag{20}$$

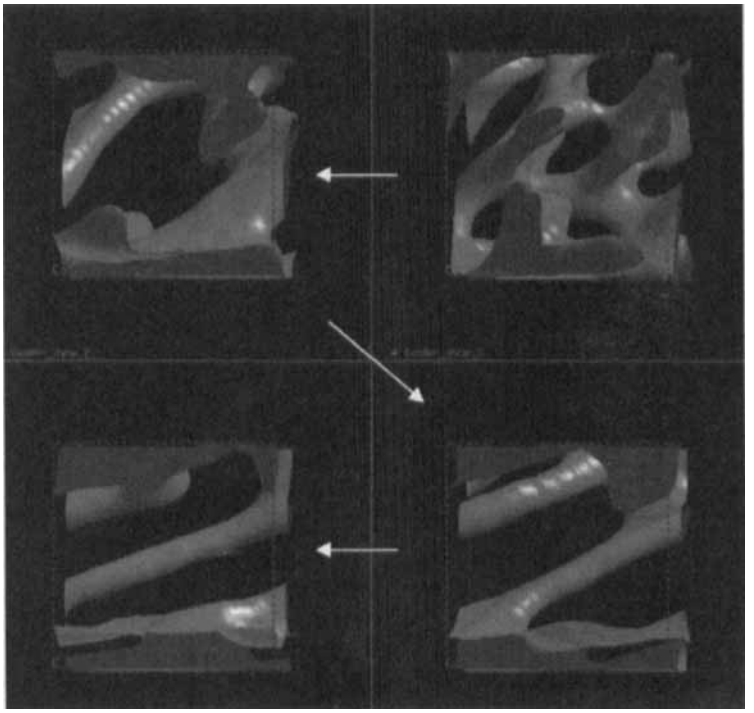

FIGURE 5 Time sequence of the morphology of the polyisoprene component of polystyrene-polyisoprene diblock copolymers at 30% concentration in the solvent di-*n*-butyl phthalate under shear. The time sequence proceeds following the arrows. The final morphology shows regions of rodlike order in coexistence with lamellar order (the lamellae, near the top and bottom of the simulation cell, are oriented normal to the picture plane). (See Color Plate X).

where μ_c is the chemical potential of the compatibiliser and Γ_c is the surface excess. The chemical potential can be found from simulation by measuring the surface excess for a given bulk concentration ϕ_c, together with an assumption that the compatibiliser is dilute

$$d\gamma = -(RT\,\Gamma_c/\phi_c)d\phi_c \tag{21}$$

A theoretical study of the isotropic phases of this system revealed the possibility of regions of three-phase coexistence [17], where the system could macro-phase separate into regions with high compatibiliser concentration, thus effectively weakening the blend. Figure 7 shows the confirmation of this prediction *via* simulation. It should be noted that for practical blend formulations this shouldn't be an issue, as the compatibiliser concentrations for which this behaviour is seen are much larger than those normally used.

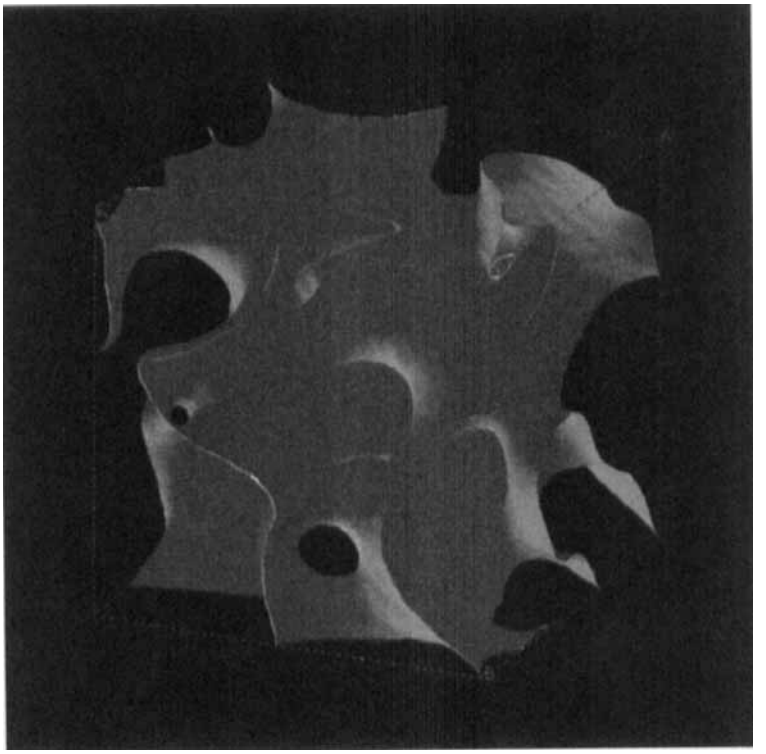

FIGURE 6a Isodensity surfaces in a polystyrene-polyisoprene (PS-PI) blend, after roughly a millisecond of demixing. The molecular weight of both polymers was taken to be roughly 80,000 g/mol. Here the blue surface encloses regions of high PS concentration, and the orange high PI concentration. (See Color Plate XI).

Ongoing work is examining the interesting behaviour which arises when the compatibiliser molecule is large compared with the homopolymers. Then, the compatibiliser can dominate the system and the demixing can be restricted to microphase separation. As more homopolymer is added, there is a crossover from micro- to macro- phase separation, at a Lifshitz point. Recent experimental work has found the polymeric equivalent of a bicontinuous microemulsion phase in this part of the phase diagram [18].

DPD

Dissipative Particle Dynamics has been applied to a tremendous range of different applications, including suspension rheology [19] and multiphase flow [20]. Here we restrict our attention to applications in the polymer area.

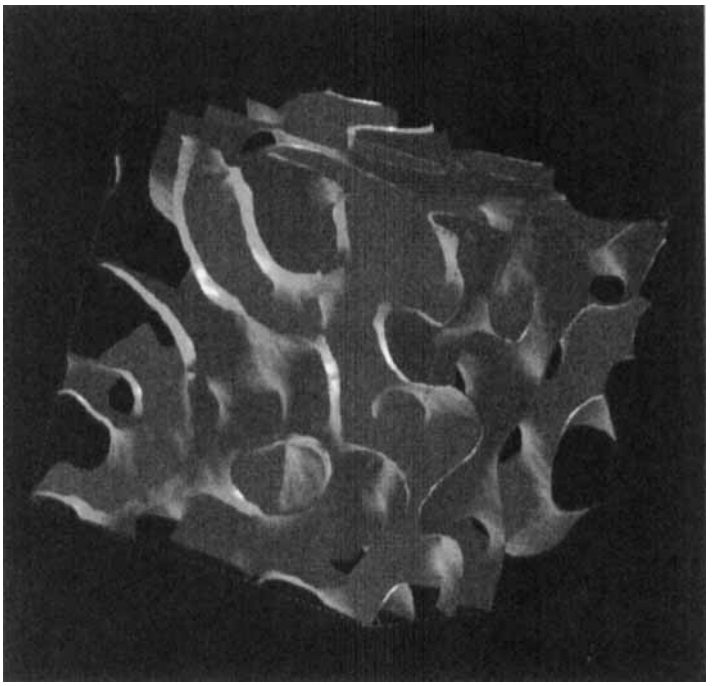

FIGURE 6b Isodensity surfaces in a polystyrene-polyisoprene blend with added compatibliser, after the same demixing time as in Figure 6a. The colour scheme is the same as that in Figure 6a. The molecular weight of both polymers was the same as in Figure 6a, and the compatibiliser was a polystyrene-polyisoprene diblock copolymer of the same molecular weight as the homopolymers. Note the much higher curvature of the compatibilised blend, due to a strong reduction in the interfacial tension. (See Color Plate XII).

Rob Groot and Tim Madden at Unilever have recently used Dissipative Particle Dynamics (DPD) to clarify the complex micro-phase separation behaviour which occurs in block copolymer systems [21].

These materials, which are essentially neat surfactants, are used in many of Unilever's product areas. Within the food category alone they may form an important ingredient in ice cream, meat snacks, margarine, cheese and frozen foods.

Groot and Madden found a correct implementation of hydrodynamics to be the essential ingredient in correctly predicting the morphologies of different systems and in understanding the complex pathway by which each system micro-phase separates. The hydrodynamic modes are responsible for large-scale collective motions of the polymers which the simulations revealed to be nematic and smectic ordering transitions.

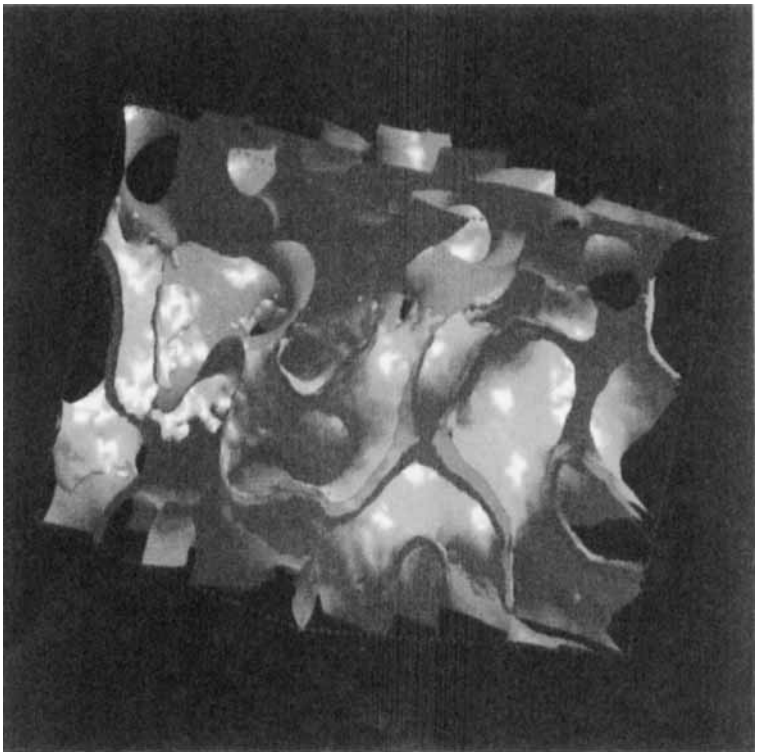

FIGURE 7 Phase separation of compatibiliser in an improperly formulated blend, with the same polymer components as in Figure 6b, but at a larger compatibiliser concentration. Here the blue surface represents the PS-PI interface, and the orange surface encloses regions of high compatibiliser concentration. The compatibiliser is seen to still prefer the interface, but is not uniformly distributed over it. (See Color Plate XIII).

Simulations at Unilever and MSL have also shown how DPD may be used to estimate critical micelle concentration and surfactant kinetics in oil-water-surfactant systems. By studying such a ternary system in a geometry where a planar interface is formed, and measuring the interfacial tension by integrating the stresses through the interface, it was possible to identify a concentration at which the surface tension dropped dramatically (see elsewhere in this volume).

By varying the system building process, it is possible to examine the kinetics of this lowering of interfacial tension. A system is constructed wherein the surfactant is wholly suspended in either the oil phase or the water phase, by artificially decreasing the Flory-Huggins interactions between some beads.

Then the interaction parameters are set to their real physical values, and the surfactant concentration profiles and interfacial tension are monitored over time. Figure 8 displays curves of interfacial tension γ *versus* simulation time for two different surfactant concentrations. The curves display an initial increase in γ over time which we attribute to the formation of an initial surfactant depletion layer near the oil-water interface. Micellisation of the surfactant also occurs, giving rise to a kinetics to which many different mechanisms must contribute.

Simulations of polymers in dilute solution and in confined geometries have been performed by Manke, Schlijper and co-workers [22, 23]. Here the interest was in including explicit solvent, so that solvent fluctuation effects could be studied, to improve on theories of viscoelasticity based on mean-field hydrodynamics. While the simulations confirmed that the modes of the DPD polymer were Rouse-like, they also exposed a novel mechanism by which the confining walls affected the polymer conformation *via* hydrodynamic modes. This has interesting possible applications in the design of lubricants.

Finally, our own work using DPD has focused on validating the method for the specific Pluronic surfactants which have been so well-studied using MesoDyn. As both simulation methods have an underlying Flory-Huggins free energy, a direct mapping between the two should be possible, *via*

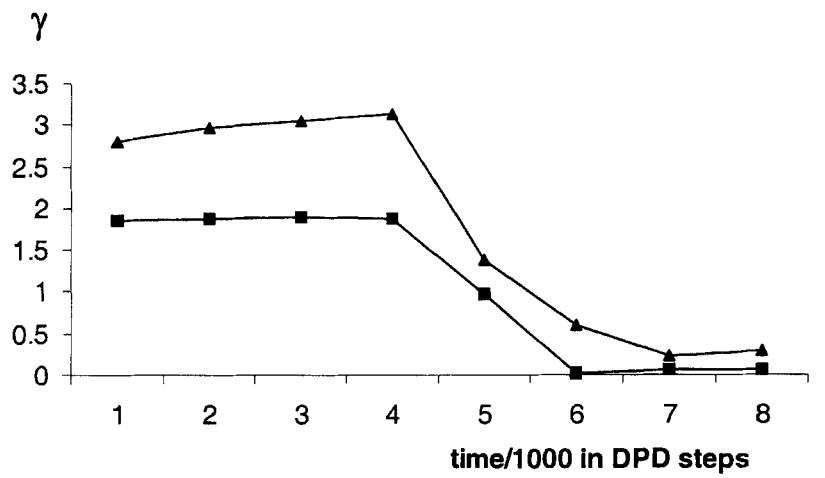

FIGURE 8 Time evolution of the interfacial tension γ in an oil-water-surfactant system. The upper curve is for a bulk surfactant concentration of 5 percent, and the lower curve for a concentration of 15 percent. The initial increase in γ we attribute to a depletion layer forming next to the oil-water interface.

equating χ parameters. Thus, the existing χ parameters for the Pluronics, which were determined by vapour pressure measurements, were used to determine the DPD repulsion parameters, and DPD simulations run at a polymer concentration of 55% , where a hexagonal phase is expected, both from experiment and MesoDyn simulations. The simulations showed that the simple mapping of DPD onto MesoDyn *via* their expressions for χ is valid, in that the DPD simulations predict the correct morphology for Pluronic surfactants under shear (see Fig. 9).

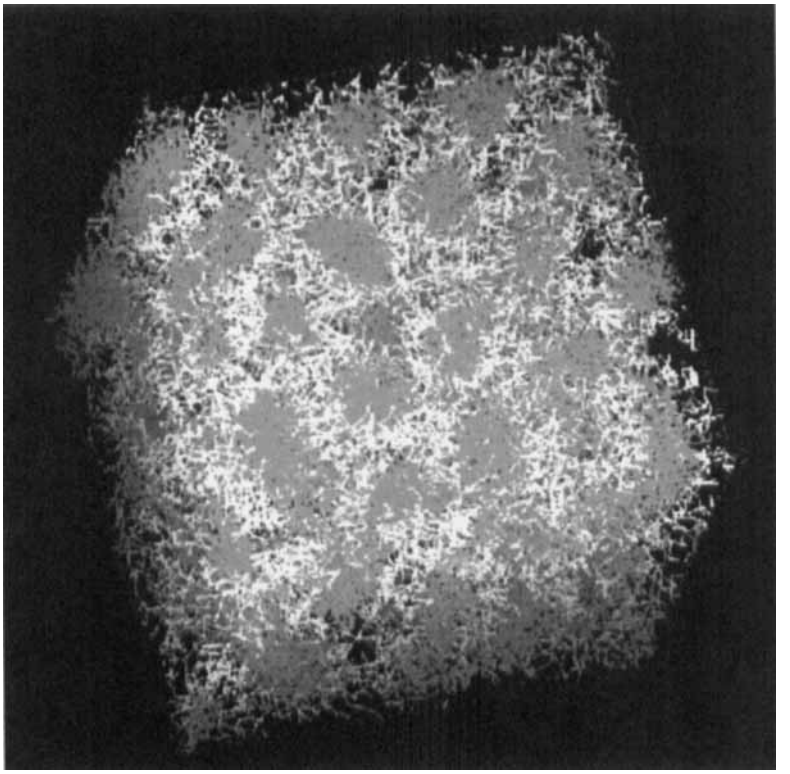

FIGURE 9 Configuration of Pluronic L64 triblock copolymer molecules at 55% concentration in water (the water is not shown), after several thousand DPD time units. The central poly(propylene-oxide) (PPO) block is displayed in yellow, and the two outer poly(ethylene-oxide) (PEO) blocks are displayed in white. The plane of shear is parallel to the left-hand cell face. Note that the morphology of the PPO blocks is hexagonal, as predicted by experiment. There is still a large amount of disorder in the hexagonal structure, but the upper part of the cell clearly shows that the triangular lattice formed by the rods has one unit vector normal to the plane of shear. (See Color Plate XIV).

Acknowledgements

I would like to thank the members of the MesoDyn Esprit project: Hans Fraaije, Andrei Zvelindovsky, Agur Sevink, Olaf Evers, Peter Altevogt, Jose Brokken, Henk Huinink, and Gunnar Nyland for discussions. MesoDyn is funded in part by the European Community, under Esprit grant #22865. I would also like to acknowledge Bernard van Vlimmeren and Natasha Maurits for valuable discussions concerning MesoDyn, and Rob Groot and Patrick Warren for improving my understanding of DPD.

References

[1] Fraaije, J. G. E. M. (1993). "Dynamic Density Functional Theory for Micro-Phase Separation Kinetics of Block Copolymer Melts", *J.Chem. Phys.*, **99**, 9202.

[2] Fraaije, J. G. E. M., van Vlimmeren, B. A. C., Maurits, N. M., Postma, M., Evers, O. A., Hoffman, C., Altevogt, P. and Goldbeck-Wood, G. (1997). "The Dynamic Mean-Field Density Functional Method and its Application to the Mesoscopic Dynamics of Quenched Block Copolymer Melts", *J. Chem. Phys.*, **106**, 4260.

[3] Maurits, N. M., Zvelindovsky, A. V. and Fraaije, J. G. E. M. "Equation of State and Stress Tensor in Inhomogeneous Compressible Copolymer Melts: Dynamic Mean-Field Density Functional Approach" (submitted to *J. Chem. Phys.*).

[4] Maurits, N. M. and Fraaije, J. G. E. M. (1997). "Mesoscopic Dynamics of Copolymer Melts: from Density Dynamics to External Potential Dynamics using Nonlocal Kinetic Coupling", *J. Chem. Phys.*, **107**, 5879–5889.

[5] Hoogerbrugge, P. J. and Koelman, J. M. V. A. (1992). "Simulating Microscopic Hydrodynamic Phenomena with Dissipative Particle Dynamics", *Europhysics Letters*, **19**, 155–160.

[6] Espanol, P. and Warren, P. (1995). "Statistical Mechanics of Dissipative Particle Dynamics", *Europhysics Letters*, **30**, 191–196.

[7] Groot, R. D. and Warren, P. B. (1997). "Dissipative particle dynamics: Bridging the gap between atomistic and mesoscopic simulation", *J. Chem. Phys.*, **107**, 4423–4435.

[8] For an explanation, see *e.g.*, Boyd, R. H. and Phillips, P. J. "The Science of Polymer Molecules" Cambridge University Press, (1993), ch.9.

[9] Alexandridis, P. *et al.* (1995). "Self-Assembly of Amphiphilic Block Copolymers: The $(EO)_{13}(PO)_{33}(EO)_{13}$ – Water – *p*-Xylene System", *Macromolecules*, **28**, 7700.

[10] van Vlimmeren, B. A. C., Maurits, N. M., Zvelindovsky, A. V., Sevink, G. J. A. and Fraaije, J. G. E. M. (1999). "Simulation of 3D Mesoscale structure formation in concentrated aqueous solution of the triblock polymer surfactants (Ethylene Oxide) 13 (Propylene Oxide) 30 (Ethylene Oxide) 13 and (Propylene Oxide) 19 (Ethylene Oxide) 33(Propylene Oxide) 19. Application of dynamic mean-field density functional theory" *Macromolecules*, **32**, 646–656.

[11] Zvelindovsky, A. V., van Vlimmeren, B. A. C., Sevink, G. J. A., Maurits, N. M. and Fraaije, J. G. E. M. "3D simulation of hexagonal phase of a specific polymer system under shear: the dynamic density functional approach", Submitted to *J. Chem. Phys.* (rapid communications).
References 3, 10 and 11 are available in preprint form from the MesoDyn Esprit Project Web site: http://www.fwn.rug.nl/mesodyn/index.html.

[12] Olaf Evers, presented at a joint MSI/IBM Seminar Series on Mesoscale Modelling, Houston, Chicago and Princeton, March 1998.

[13] Hamley, I. W. *et al.* (1998). "Micellar Ordering in Concentrated Solutions of Di- and Triblock Copolymers in a Slightly Selective Solvent", *Macromolecules*, **31**, 1188.

[14] Matsen, M. W. and Bates, F. S. (1996). "Unifying Weak- and Strong-Segregation Block Copolymer Theories", *Macromolecules*, **29**, 1091–1098.

[15] Zvelindovsky, A. V. personal communication.
[16] Leibler, L. (1982). "Theory of Phase Equilibria in Mixtures of Copolymers and Homopolymers. 2. Interfaces near the Consolute Point", *Macromolecules*, **15**, 1283.
[17] Broseta, D. and Fredrickson, G. H. (1990). "Phase equilibria in copolymer/homopolymer ternary blends: Molecular weight effects", *J. Chem. Phys.*, **93**, 2927.
[18] Bates, F. S. *et al.* (1997). "Polymeric Bicontinuous Microemulsions", *Phys. Rev. Lett.*, **79**, 849.
[19] Boek, E. S., Coveney, P. V., Lekkerkerker, H. N. W. and van der Schoot, P. (1997). "Simulating the rheology of dense colloidal suspensions using dissipative particle dynamics", *Phys. Rev. E*, **55**, 3124–3133.
[20] Coveney, P. V. and Novik, K. (1996). "Computer simulations of domain growth and phase separation in two-dimensional binary immiscible fluids using dissipative particle dynamics", *Phys. Rev. E*, **54**, 5134–5141.
[21] Groot, R. D. and Madden, T. J. (1998). "Dynamic simulation of diblock copolymer microphase separation", *J. Chem. Phys.*, **108**, 8713.
[22] Schlijper, A. G., Hoogerbrugge, P. J. and Manke, C. W. (1995). "Computer simulation of dilute polymer solutions with the dissipative particle dynamics method", *J. Rheol.*, **39**, 567–579.
[23] Kong, Y., Manke, C. W., Madden, W. G. and Schlijper, A. G. (1994). "Simulation of a Confined Polymer in Solution Using the Dissipative Particle Dynamics Method", *International Journal of Thermophysics*, **15**, 1093–1101.